Report on PATHOS Deliverable D2.6:

Modification of spectral density by dynamical decoupling

Dieter Suter
Fakultät Physik, Technische Universität Dortmund, D-44221 Dortmund, Germany

I. MOTIVATION AND PRINCIPLES

PATHOS was conceived to develop radically new technology for the sensing of bio-systems and in-vivo diagnostics of biomedical conditions using hitherto unexploited tools of unconventional complex-system dynamical control and information sampling/ processing. Knowledge of the noise characteristics of these systems is important for understanding and predicting their evolution. The two main motivations for a detailed analysis of the noise properties are (i) to develop techniques that reduce the unwanted effect of the noise on the system of interest [1–3] and (ii) to extract useful information about the environment that generates the noise [4–7].

This approach is proving is particularly useful in the context of MRI, where the different relaxation times offer the best option for contrast between different type of tissue as well as for assessing the health status and physiological properties of different tissues [8, 9] and in optically detected magneetic resonance (ODMR), as pointed out in the project proposal. In the context of quantum technologies, knowledge of the properties of the environmental noise can be helpful for assessing and mitigating its deleterious effect on the superposition states that are the essential ingredients of most quantum technologies. PATHOS specifically uses nitrogen-vacancy (NV) centers in diamond as near quantum-limited sensors.

Modifying the spectral distribution can reduce the unwanted effects and extract useful information about the environment [1, 4]. Suitable modulation schemes can also generate back-action on the environment: The modulated interaction drives not only the system, but equally the environmental degrees of freedom. It can therefore be used, e.g., to control nuclear spins that are coupled to an electron spin via hyperfine interaction [10]. The modulated hyperfine coupling can then be used to drive the nuclear spins, with a much higher efficiency than what can be achieved by direct control via radio-frequency pulses [11–14] . Modulation can be pulsed such as dynamical decoupling (DD) [1] or continuous control fields [15, 16]. In this review, we focus the DD scheme.

II. EVOLUTION AND DEPHASING

The basic concept of noise spectroscopy has two actors: the system, probe or sensor that is used for the monitoring and an environment that is the source of the noise. In the following, we will make the assumption that we have complete control over the system degrees of freedom but only limited or no control over the environment. While any quantum mechanical system can be used as the probe, we will focus here on the simplest type, i.e., a two-level system, often known as a qubit or a (pseudo-) spin 1/2. Other options include multiple qubits, higher spins (e.g. spin 1 or spin 3/2) or harmonic oscillators [7].

A. System and operators

We first consider a quantum system with a static Hamiltonian that interacts with its environment. The total Hamiltonian of the system and the environment can be represented as [1, 17]

$$\mathcal{H} = \mathcal{H}_S + \mathcal{H}_E + \mathcal{H}_{SE}. \quad (1)$$

Here $\mathcal{H}_S$ is the static or natural Hamiltonian of the system of interest $\mathcal{H}_E$ and $\mathcal{H}_{SE}$ are refer to the environment and the system-environment interaction with

$$\mathcal{H}_{SE} = \sum_j d_j A_j \otimes B_j \quad (2)$$

where d_j is the coupling constant for the term with index j and A_j and B_j are operators acting on the system and the environment.

Since system and environment are independent degrees of freedom, the corresponding operators commute:

$$[\mathcal{H}_S, \mathcal{H}_E] = [A_j, B_k] = 0$$

for all j, k.

B. Time dependence

Here, we consider the time dependence of an operator A acting on the system degrees of freedom. The full time dependence can be evaluated in two stages: the evolution under the system Hamiltonian $\mathcal{H}_S$ and the additional evolution under the system-environment operator $\mathcal{H}_{SE}$. The first part can formally be written as

$$A(t) = U_S(t) A(0) U_S^\dagger(t), \quad (3)$$

where $U_S(t) = e^{-i\mathcal{H}_S t}$ and we have used the assumption that the system operator $\mathcal{H}_S$ is time-independent.

In addition to the evolution under the system Hamiltonian, the interaction with the environment makes a contribution. For a static coupling operator $\mathcal{H}_{SE}$ alone, this can be taken into account by an additional term in equation (3). However, since $\mathcal{H}_{SE}$ depends on bath- as well as systems degrees of freedom, it generates a time evolution of system operators like A that is not confined to the Hilbert space of the system: $e^{-i\mathcal{H}t}Ae^{it}$ is in general no longer a pure system operator, but it includes environmental degrees of freedom. For simplicity, one usually disregards the environmental degrees of freedom by taking the trace over the Hilbert space of the environment. This results in general in a non-unitary evolution with increasing entropy in the system density operator.

However, real environments are never completely static, and the time-dependence of the system-environment interaction is the main concern in this context. It is in general possible to distinguish two contributions to the time-dependence: through classical random variables like the position of a molecule and through evolution under the Hamiltonian. The latter can be taken into account by working in an interaction representation with respect to the main Hamiltonians $\mathcal{H}_S + \mathcal{H}_E$. In this representation, the coupling operator acquires the time dependence

$$\mathcal{H}^i_{SE}(t) = e^{-i(\mathcal{H}_S+\mathcal{H}_E)t}\mathcal{H}_{SE}e^{i(\mathcal{H}_S+\mathcal{H}_E)t}. \tag{4}$$

The time dependence of the classical variables can usually be brought into the form of time-dependent coupling constants $d_j(t)$ in equation (2). This type of time dependence occurs through processes that are not represented by the Hamiltonian $\mathcal{H}_E$. Typical examples are the molecular motion in liquids, which modulates the distance between different spins and therefore the dipolar coupling constants between them or, in the case of charged qubits, the Coulomb interaction.

In most cases (and all cases that we consider here), it is possible and useful to combine the two sources of time dependence by tracing over the environmental degrees of freedom and only considering an effective random field

$$\delta(t) = \sum_j d_j(t)\frac{\langle B_j(t)|B_j(0)\rangle}{\langle B_j(0)|B_j(0)\rangle}, \tag{5}$$

which combines the classical time dependence $d_j(t)$ with the quantum-mechanical time dependence of the bath operators $B_j(t)$. This is known as the semiclassical approach.

The time-dependence can also be generated artificially, e.g. by ancilla qubits that serve as a model environment [18].

C. Dephasing by random environment

Relaxation processes driven by environmental noise were first discussed in 1947 by Bloembergen, Purcell and Pound [19, 20]. A general theory of relaxation processes was introduced in 1957 by Redfield [17]. While this was initially developed and tested for nuclear spin systems, it soon became clear that the basic physics are the same for other quantum systems, in particular for all types of 2-level systems [21] or qubits.

We consider first the most relevant and relatively simple case where the external noise commutes with the static system Hamiltonian and acts independently on the individual qubits of the system. This corresponds to the case of pure dephasing, where the populations of the system remain constant. As discussed above, the time dependence of the system-bath coupling can then be summarised as

$$\mathcal{H}_{SE} = \sum_j \delta_j(t) S_{z,j} \tag{6}$$

where δ_j is the coupling strength acting on the $z-$component of qubit j and we choose the z-axis as the quantization axis of the system.

In the case of a single qubit, we describe the system by the density operator ρ, which we expand in terms of the spin operators S_α, $\alpha = (x, y, z)$:

$$\rho(t) = \frac{1}{2}\mathbf{1} + x(t)\, S_x + y(t)\, S_y + z(t)\, S_z.$$

The random perturbation therefore adds a phase factor

$$e^{i\varphi(t)} = e^{i\int_0^t \delta(\tau)\,d\tau}$$

to the off-diagonal elements. If the mean of the random perturbation vanishes and we work in an interaction representation that removes the evolution under the system Hamiltonian, the coefficients $x(t)$ and $y(t)$ decay as

$$\frac{x(t)}{x(0)} = \frac{y(t)}{y(0)} = \langle\cos\varphi(t)\rangle.$$

If the memory time of the environment is shorter than the time scale over which the system dephases, it is sufficient to expand the cosine to second order,

$$\begin{aligned}\langle\cos\varphi(t)\rangle &= 1 - \frac{1}{2}\langle\varphi^2(t)\rangle + \ldots \\ &= 1 - \frac{1}{2}\langle\left(\int_0^t \delta(\tau)\,d\tau\right)^2\rangle. \end{aligned} \tag{7}$$

The evolution of the phase $\varphi(t) = \int_0^t \delta(\tau)\,d\tau$ is typically a diffusion-like process whose mean square $\langle\varphi^2(t)\rangle$ increases linearly in time as

$$\langle\varphi^2(t)\rangle = \langle\delta^2\rangle\sqrt{\pi}\tau_c t. \tag{8}$$

Here, $\langle\delta^2\rangle$ is the mean square of the noise and τ_c its correlation time.

Figure 1 illustrates this behaviour with a numerical simulation of the evolution of the qubit phase for 10 different randomly generated noise traces. Each noise trace was generated by a pseudo-random generator, with a bandwidth of 1, an rms noise amplitude $\delta_{rms} = \sqrt{\langle\delta^2\rangle} = 0.355$

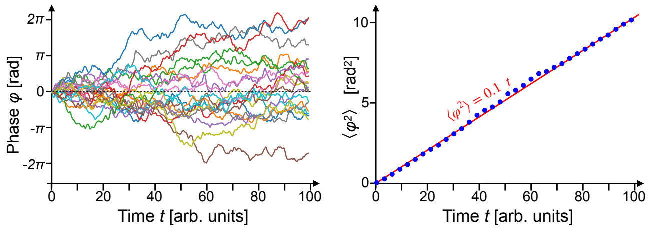

FIG. 1: Left: Evolution of the qubit phase $\varphi(t)$ for 10 different randomly generated noise traces with a bandwidth of 1, resulting in an rms noise amplitude $\delta_{rms} = \sqrt{\langle \delta^2 \rangle} = 0.355$ in arbitrary units and a correlation time $\tau_c = \sqrt{2}/\pi \approx 0.45$, also in arbitrary units. Right: Evolution of the mean square $\langle \varphi^2(t) \rangle$ of the phase. The circles were obtained by averaging over 100 different randomly generated noise traces with a bandwidth of 0.5, an rms noise amplitude $\delta_{rms} = \sqrt{\langle \delta^2 \rangle} = 0.25$, and a correlation time $\tau_c \approx 0.9$, all in arbitrary units. The straight line has the theoretical slope of 0.1.

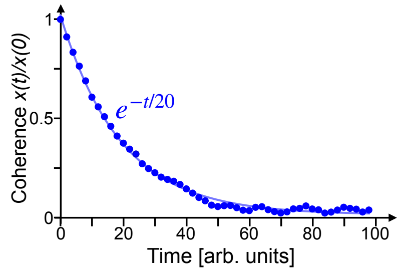

FIG. 2: Decay of the coherence $x(t)/x(0)$ calculated by averaging over 100 noise traces. The simulated points (blue circles) are compared to the exponential decay with a time constant $T_2 = 20$.

and a correlation time $\tau_c = \sqrt{2}/\pi \approx 0.45$, all in arbitrary units. The range of phases in the ensemble increases roughly with the square root of time. This is shown more clearly in the right-hand part of Fig. 1, where the points represent the mean square $\langle \varphi^2(t) \rangle$ of the phase as a function of time. The circles were obtained by averaging over 100 different randomly generated noise traces with a bandwidth of 0.5, an rms noise amplitude $\delta_{rms} = \sqrt{\langle \delta^2 \rangle} = 0.25$, and a correlation time $\tau_c \approx 0.9$, all in arbitrary units. They are compared to a straight line with the theoretical slope 0.1.

In the limit of short correlation time τ_c of the environment that we consider here, the decay of the coherence per unit time is constant and therefore the overall decay follows an exponential,

$$\frac{x(t)}{x(0)} = \frac{y(t)}{y(0)} = \langle \cos \varphi(t) \rangle = e^{-t/T_2}. \tag{9}$$

Comparing eqs (7) and (9) for short times, $t \ll T_2$, we find

$$T_2 = \frac{2t}{\langle \left(\int_0^t \delta(\tau)\, d\tau \right)^2 \rangle}. \tag{10}$$

Using (8) we obtain

$$T_2 = \frac{2}{\langle \delta^2 \rangle \sqrt{\pi} \tau_c}.$$

Figure 2 illustrates this with a numerical example with $\delta_{rms} = \sqrt{\langle \delta^2 \rangle} = 0.355$ and $\tau_c = \sqrt{2}/\pi \approx 0.45$ in arbitrary units. They are compared to an exponential decay with the expected decay time of $T_2 = 20$.

III. REFOCUSING

As discussed above, noise tends to degrade the information contained in the quantum system. On the other hand, it is also a very important source of information about the environment [22, 23]. Being able to control it, e.g. to minimise it or to suppress specific parts of it, is therefore an important goal for a diverse range of fields [1, 4, 24–27]. In this chapter we first discuss the basic properties of refocusing, while the following chapter will focus on techniques that are more selective for specific components of the noise.

A. Echoes

Section II C provided a discussion of the dephasing due to environmental noise, as it occurs in any quantum mechanical system. This behavior can be modified by additional control fields that interact with the system and / or the environment. A typical case of a control field acting on the environment is that of heteronuclear decoupling used in NMR [25, 26, 28, 29]. Here, we focus on systems where the environment can not be controlled, so the control operations can only act on the system degrees of freedom.

A relatively simple and very common scheme for modifying the system-environment interaction by operations on the system is to apply a so-called refocusing-pulse to the system. The earliest example of this case is the spin-echo, which was first observed by Erwin Hahn [30] and quickly extended to other systems, such as optical transitions [31], where it is known as a photon echo.

Figure 3 shows schematically the pulse sequence and the evolution of the system for the generic case of a time-independent perturbation given by the Hamiltonian

$$\mathcal{H}_{SE} = \delta S_z.$$

As discussed in section II, this interaction multiplies the coherence of the qubit by the phase factor

$$e^{i\varphi(\tau)} = e^{i \int_0^\tau \delta(t)\, dt}$$

during an evolution of duration τ. An ideal refocusing pulse applied at time τ transforms the density operator as

$$\rho(\tau+) = e^{i\pi S_y} \rho(\tau-) e^{-i\pi S_y},$$

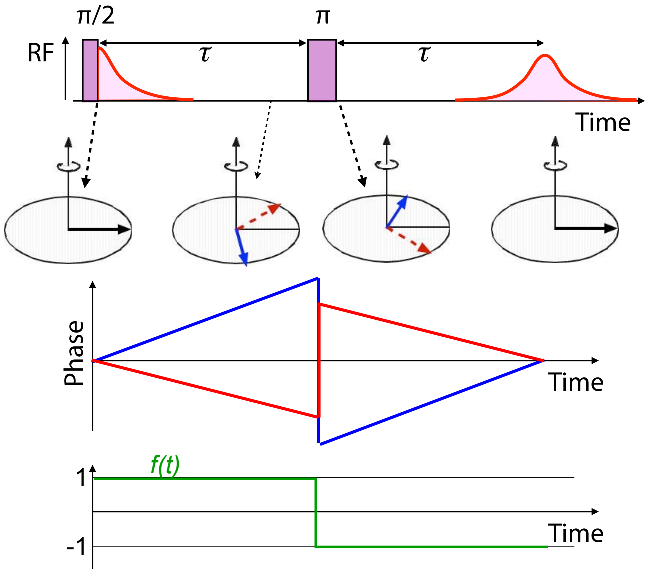

FIG. 3: Top: pulse sequence for refocusing coherence. The blue and red arrows indicate the evolution of coherence packages in different environments in the xy-plane. The second trace shows the corresponding phase as a function of time. The third trace shows the modulation function $f(t)$ as a function of time.

which corresponds to an inversion of the phase, $\varphi(\tau+) = -\varphi(\tau-)$. Here, $\tau-$ and $\tau+$ represent the state of the system immediately before and after the refocusing pulse which is approximated here by an ideal δ-function.
After the refocusing pulse, the system evolves under the same Hamiltonian and therefore acquires additional phase at the same rate. The total acquired phase at time 2τ can then be written as

$$\varphi(2\tau) = -\int_0^{2\tau} f(t)\,\delta(t)\,dt,$$

where $f(t)$ is the sign modulation function Suter and Álvarez [1], Kofman and Kurizki [32] that tracks the effective coupling strength through the sequence. For an ideal δ-function refocusing pulse, the sign modulation function of the Hahn echo is

$$f(t) = \begin{cases} +1 & 0 \le t \le \tau \\ -1 & \tau \le t \le 2\tau \end{cases},$$

as shown in the bottom part of fig. 3.
Figure 3 tracks this behavior for a static environment, where δ is constant in time, for two different values of δ, marked by the red and blue lines. Both lines meet at $\varphi(2\tau) = 0$, indicating that the resulting phase is independent of the specific state of the environment. Accordingly, while the evolution depends on the state of the environment, the final state of the system at $t = 2\tau$ does not. If we average over many realisations of the environment (either by repeating the experiment or by working with ensembles), the average coherence of the system reaches a maximum at this point, as evidenced by the echo at $t = 2\tau$.
Another way of describing the evolution is to transform the Hamiltonian into the "toggling-frame" representation [33–35], where the Hamiltonian is

$$\tilde{\mathcal{H}}(t) = U^{-1}(t)\mathcal{H}U(t)$$

and the transformation operator

$$U(t) = \mathcal{T}\,exp[-i\int_0^t \mathcal{H}^c(t')dt'].$$

Here, $\mathcal{T}$ is the Dyson time-ordering operator and $\mathcal{H}^c$ is the control Hamiltonian generating the refocusing pulse(s).

B. Fluctuating environment

For a static environment, such echo experiments with an ideal inversion pulse can completely refocus the dephasing due to the environment. This is no longer the case when the environment changes before the echo is formed.

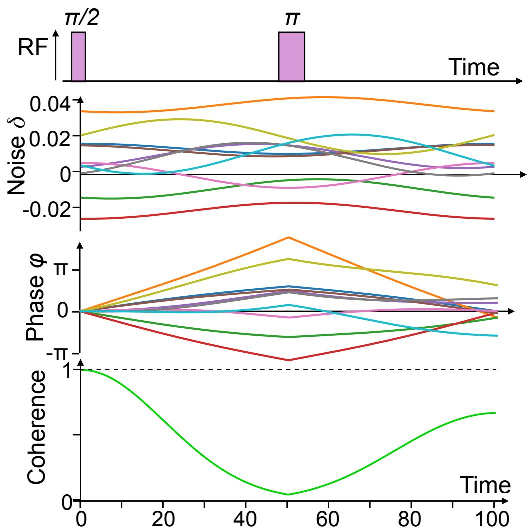

FIG. 4: Incomplete echo formation in a slowly time-dependent environment. The top trace shows the pulse sequence, the second trace the slowly varying noise field for 10 different random environments, the third trace the evolution of the phase $\varphi(t)$ of the qubit for the same realisations of the environment, and the bottom the coherence $\langle\cos\varphi(t)\rangle$, averaged over 1000 random, time-dependent environments.

Figure 4 illustrates this case with a numerical example: Since each realisation of the noisy environment varies with time, the slope of the phase versus time is not constant and the accumulated phase at $t = 2\tau$ is not zero. As a consequence, the echo signal is smaller than the initial coherence. For this example, an RMS noise of $\delta_{RMS} = \sqrt{\langle\delta^2\rangle} = 0.008$ was used, with τ_c=56.

For a more quantitative analysis, we start with the assumptions of sec. II C, and calculate the evolution of the phase $\varphi(t) = \int_0^t \delta(\tau)\,d\tau$ under the effect of the modulated noise $\delta'(\tau) = \delta(\tau)f(\tau)$ up until the time τ_E of the echo as

$$\begin{aligned} \varphi(\tau_E) &= \int_0^{\tau_E} \delta'(\tau)\,d\tau \\ &= -\int_0^{\tau_E/2} \delta(t)\,dt + \int_{\tau_E/2}^{\tau_E} \delta(t)\,dt. \end{aligned} \tag{11}$$

As in section II, its average vanishes, $\langle\varphi\rangle = 0$, but the variance $\langle\varphi^2\rangle$ is nonzero.
A useful way of evaluating the integral consists in decomposing the noise into a Fourier series:

$$\begin{aligned} \delta(t) &= \frac{\delta_0}{2} + \sum_{k=1}^{\infty}(a_k \cos\frac{k\,2\pi\,t}{\tau_E} + b_k \sin\frac{k\,2\pi\,t}{\tau_E}) \\ &\approx \delta(0) + a_1 \cos\frac{2\pi\,tt}{\tau_E} + b_1 \sin\frac{2\pi\,t}{\tau_E}, \end{aligned}$$

which can be terminated after the first order term for slowly varying noise. This will be a good approximation for $\tau_c > \tau_E$, which is the condition for an effective refocusing. At the same time, it represents the minimal spectral decomposition of the noise.
Inserting this Fourier series into (11), we get

$$\begin{aligned} \varphi(\tau_E) &= -\int_0^{\tau_E/2} \delta(t)\,dt + \int_{\tau_E/2}^{\tau_E} \delta(t)\,dt. \\ &= -2b_1\frac{\tau_E}{\pi}. \end{aligned}$$

So the remaining phase is directly proportional to the coefficient b_1 of the Fourier series. Within this approximation, the variance becomes

$$\langle\varphi^2(\tau_E)\rangle = \frac{4}{\pi^2}\langle b_1^2\rangle\tau_E^2,$$

i.e., the even terms (constant and cos) are refocused, but the odd (sin) term remains. For the range of validity, where $\langle\varphi^2\rangle \ll 1$, the attenuation of the echo is then

$$\begin{aligned} \langle\cos\varphi(\tau_E)\rangle &= 1 - \frac{1}{2}\langle\varphi^2(\tau_E)\rangle \\ &= 1 - \frac{2}{\pi^2}\langle b_1^2\rangle\tau_E^2. \end{aligned}$$

Clearly, this does not correspond to an exponential decay, but for short times it can be compared to a Gaußian,

$$\langle\cos\varphi(t)\rangle = 1 - \frac{2}{\pi^2}\langle b_1^2\rangle\tau_E^2 = e^{-\tau_E^2/T_2^2} \approx 1 - \frac{\tau_E^2}{T_2^2},$$

which yields

$$T_2 = \frac{\pi}{\sqrt{2}}\sqrt{\langle b_1^2\rangle}.$$

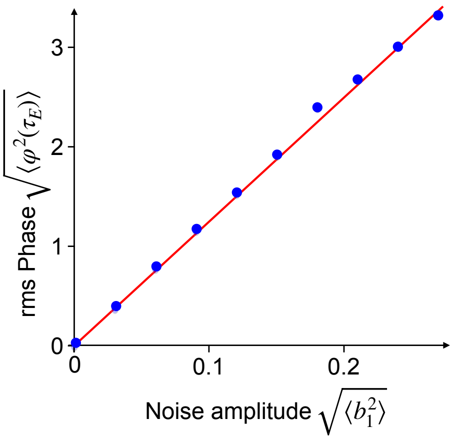

FIG. 5: $\sqrt{\langle\varphi^2\rangle}$ vs. b_1. The fit shows $\sqrt{\langle\varphi^2\rangle} = 126\,b_1$.

Figure 5 shows a numerical test for an echo time $\tau_E = 200$. We therefore expect

$$\sqrt{\langle\varphi^2\rangle} = \frac{4}{\pi^2}\tau_E^2 b_1 \approx 127\,b_1$$

in excellent agreement with the fit.
Since the echo amplitude decreases quadratically with τ_E and with the noise amplitude b_1 at $\frac{2\pi}{\tau_E}$, which increases with τ_E, the echo amplitude decreases much more rapidly with increasing pulse separation than in the case of free precession.

$$\begin{aligned} \langle\cos\varphi(t)\rangle &= 1 - \frac{2}{\pi^2}\langle b_1^2\rangle\tau_E^2 = 1 - \frac{2}{\pi^2}\delta_0^2\tau_E^2 e^{-16\pi^2/(b^2\tau_E^2)} \\ &= e^{-\tau_E^2/T_2^2} \approx 1 - \frac{\tau_E^2}{T_2^2}. \end{aligned}$$

In the range of validity $\langle b_1^2\rangle\tau_E^2 \ll 1$, the decay of the coherence matches that of a Gaußian. We therefore describe the later decay with a Gaußian, with

$$T_2 = \frac{\pi}{\sqrt{2\langle b_1^2\rangle}},$$

which has the same behaviour in the short-time limit.

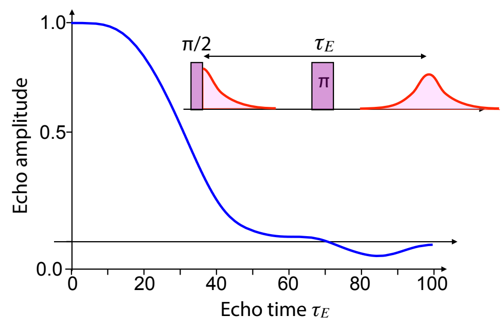

FIG. 6: Simulated decay of the Hahn-echo in a fluctuating environment.

Figure 6 shows how the echo amplitude changes with the time from the initial excitation to the echo. The trace was simulated by generating noise traces and calculating the evolution during the Hahn echo experiment for every trace and adding the results. It also shows that the echoe does not decay exponentially with the echo time but has initially a very slow decay.

C. Multiple echo sequences (CPMG)

As shown in Fig. 6, the refocusing efficiency drops when the refocusing pulse is applied after a time that is comparable or bigger than the correlation time of the environmental noise. Preserving coherence for longer times can therefore only be achieved if the refocusing is repeated, using a series of refocusing pulses with delays that are short compared to the correlation time τ_c of the environment, $\tau \ll \tau_c$. This scheme was introduced in magnetic resonance by Carr and Purcell [36] and later modified by Meiboom and Gill [37]. In the context of quantum information processing, it became known as dynamical decoupling [38].

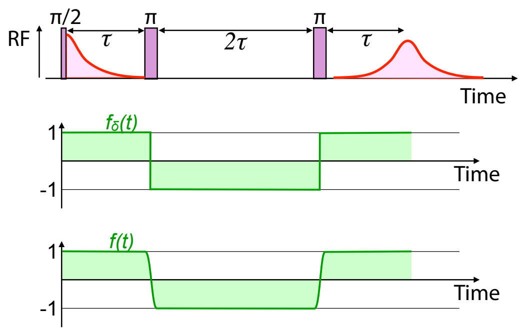

FIG. 7: A simple dynamical decoupling sequence with 2 refocusing pulses, together with the switch function $f(t)$ for ideal and for finite refocusing pulses.

Figure 7 illustrates this for the simplest cyclic DD sequence, consisting of two π pulses. Figure 8 shows an experimentally measured sequence of nuclear spin echoes during a CPMG sequence.

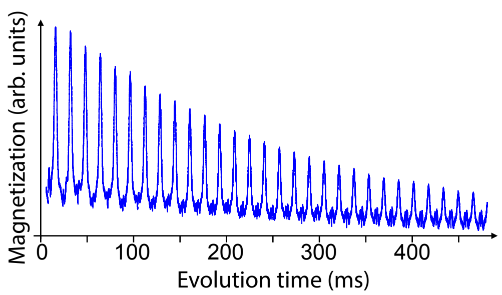

FIG. 8: Nuclear spin magnetisation during a CPMG sequence.

In the case of the single spin echo, the dominant decay mechanism was due to the Fourier component of the noise whose period is equal to the duration τ_E of the sequence. In the case of multiple echoes, it is still possible to identify specific frequency components in the noise that make the dominant contribution. The relevant components can be calculated from the Fourier transform of the pulse sequence. Using again eq. (7) to calculate the echo amplitude,

$$\langle \cos \varphi(t) \rangle \;\approx\; 1 - \frac{1}{2} \langle \left(\int_0^t \delta'(\tau)\, d\tau \right)^2 \rangle,$$

but using the effective noise $\delta'(\tau) = \delta(\tau) f(\tau)$. Since $\delta(\tau)$ is a random process, so are $\delta'(\tau)$ and its integral. On average, $\delta'^2(\tau)$ does not depend on τ, i.e. we can assign it a mean value $\langle \delta'^2(\tau) \rangle = {\delta'_{rms}}^2$, which also corresponds to the maximum of the correlation function

$$G(t_1, t_2) = \overline{\delta(t_1)\delta(t_2)},$$

where we have assumed that δ is real-valued, depends only on the difference $\tau = t_2 - t_1$ and is symmetric in time: $G(\tau) = G(-\tau)$.
The Fourier transform of the correlation function is the power spectral density

$$J(\omega) \;=\; \int_{-\infty}^{\infty} G(\tau) e^{-i\omega\tau} d\tau.$$

Therefore the rms value of the noise is given by the integrated power spectral density

$${\delta'_{rms}}^2 = \int_{-\infty}^{\infty} J(\omega) d\omega.$$

This makes it possible to write the the variance of the phase as

$$\langle \varphi^2(T) \rangle = \sqrt{2\pi} \int_{-\infty}^{\infty} |F(\omega, T)|^2 J(\omega) d\omega,$$

where $J(\omega)$ is the spectral density of the (unmodulated) environment and $F(\omega, T)$ is the finite time Fourier transform of the switching function from the excitation pulse at $t = 0$ to the endo of the echo sequence at $t = T$. This forms the basis of the spectral filter approach to be discussed in the following section.

IV. SPECTRAL FILTERS

A. Free precession and echoes

In this section, we consider filters for noise, i.e., effects of experimental techniques that modulate the interaction between system and environment by generating effective filter functions $F(\omega, T)$ - either for reducing decoherence, i.e. maximizing $\langle \varphi^2(T) \rangle$, or for spectral analysis, to probe $J(\omega)$. The term “filter” compares this

frequency-dependent attenuation of the noise to electrical filter theory [39]. The filters can be present in the system naturally, or they can be imposed by external controls.
The simplest case is that of free precession. Using the rotating frame, where only the effect of the noise has to be considered, the time-domain filter function is equal to unity for all times. The frequency domain filter function becomes therefore

$$F_{FID}(\omega, T) = \sin^2(\omega T/2).$$

For the Hahn-echo, the filter function is

$$F_{Hahn}(\omega, T) = |1 - 2e^{i\omega T/2} + e^{i\omega T}|^2.$$

At low frequency, $\omega T \approx 0$, $F_{Hahn}(\omega T) \approx 0$, meaning that the Hahn-echo can refocus low frequency components completely.

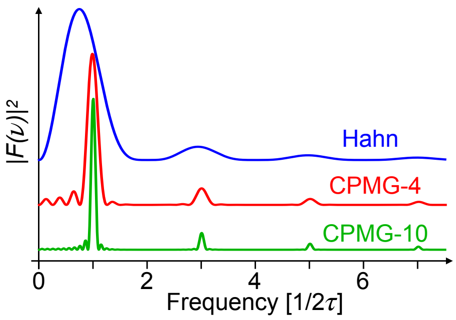

FIG. 9: Filter functions for different echo sequences.

Next we consider a sequence of N ideal inversion pulses, separated by delays τ, which is known as the Carr-Purcell [36] or CPMG [37] sequence in magnetic resonance or dynamical decoupling (DD) sequence [38] in quantum information. Figure 9 shows the corresponding filter functions for a Hahn echo and for CPMG sequences with 4 and 10 refocusing pulses. The delay between the refocusing pulses is 2τ.

B. Population-relaxation

The simplest version of a noise filter is obtained if one considers equilibration of populations through relaxation, rather than the dephasing of coherence. This process was first described by Einstein in his quantum theory of radiation [40] and for nuclear spins by Bloembergen, Purcell and Pound [19, 20], with more details given, e.g., in Refs [17, 41].
The case of population relaxation can be obtained from eq. (4) by considering coupling operators $\mathcal{H}_{SE}$ that do not commute with the system Hamiltonian $\mathcal{H}_S$. For the generic case of a single qubit, where $\mathcal{H}_S = -\omega_0 S_z$,we can then choose $\mathcal{H}_{SE} = S_x \sum_j d_j(t) B_j$, using the same notation as in section II: the time dependence of the coupling strength refers to the classical variables like the position and orientation of the molecule, while the time dependence of the bath operators are determined by the evolution under the bath Hamiltonian $\mathcal{H}_E$. Eq. (4) can then be written as

$$\mathcal{H}^i_{SE}(t) = \delta(t)(S_x \cos\omega_0 t - S_y \cos\omega_0 t),$$

where $\delta(t)$ is defined in eq. (5) and we have chosen the x-axis to point along the perturbation. With this interaction, the transition rate becomes

$$r = \int_0^t \langle \delta(0)\delta(\tau)\rangle \cos\omega_0\tau \, d\tau.$$

In all relevant cases of population relaxation, the time scale over which the system changes appreciably is long compared to the correlation time τ_c over which the correlation function $\langle \delta(0)\delta(\tau)\rangle$ decays to zero. It is then permissible to extend the upper limit of the integral to infinity, which turns the integral into a Fourier transform. The decay rate T_1^{-1} of the population difference is therefore also given by the power spectral density, but in contrast to the case of pure dephasing, it's value has to be evaluated at the transition frequency ω_0:

$$\frac{1}{T_1} = \int_0^\infty \langle \delta(0)\delta(\tau)\rangle \cos\omega_0\tau \, d\tau, \qquad (12)$$

in agreement with [19, 20]. The filter function is therefore a delta function at the transition frequency.
This important and very general result has a very simple physical interpretation: The system is a (very narrow-band) filter for the noise, it only responds to the component at the transition frequency, which is related to the energy difference between the two system levels by Bohr's resonance condition, $\Delta\mathcal{E} = \hbar\omega_0$. For the typical case where the correlation function of $\delta(t)$ decays exponentially with characteristic time τ_c, this results in

$$\frac{1}{T_1} = \langle \delta^2 \rangle \frac{1}{1 + \omega_0^2\tau_c^2}.$$

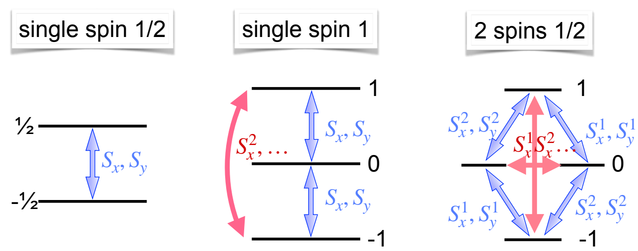

FIG. 10: Level schemes and transitions relevant for energy relaxation in these systems.

In systems consisting of more than 1 qubits / spins, relaxation can occur through different pathways at different rates. Figure 10 shows, as examples, the relevant level schemes for a single spin 1/2, a single spin 1 and a pair of spins $S = 1/2$. In each case, the transitions that can be induced by external noise sources are marked with double arrows and labelled with some of the system operators to which they couple. The relevant transition frequencies are either the Larmor frequency ω_0 or an integer (0, 2) multiple of the Larmor frequency. In all these cases, the energy level splitting (which is mostly due to the Zeeman interaction with the magnetic field) acts as a filter for the external noise: only components that fluctuate at integer multiples of the Larmor frequency have a significant effect.

This is often used to probe the spectral characteristics of noise by comparing relaxation rates at different magnetic field strengths [42, 43]. It can be extended to small fields by varying the magnetic field, which is known as field cycling [42], but also by measuring the relaxation time $T_{1\rho}$ in the rotating frame (see section **??**), where the relevant frequency is the Rabi frequency rather than the Larmor frequency [34, 44]. This approach makes the frequency range below 1 MHz accessible for experimental studies and requires only easily accessible instrumental capabilities. The filter function for these experiments can be written as

$$F_\rho(\omega; T) = \frac{\sin^2[(\omega - \omega_1)T/2]}{2\pi T(\omega - \omega_1)^2}. \tag{13}$$

C. Molecular diffusion

Molecular diffusion in a gradient can also be treated as a noisy environment [45–47]. In this case, displacement spectral density $S(\omega)$ is the Fourier transform of the velocity-autocorrelation function,

$$S_d(\omega) = \frac{D_0\tau_c^2}{\pi(1+\omega^2\tau_c^2)} = \int_{-\infty}^{\infty} \langle v(0)v(t)\rangle e^{-i\omega t} dt. \tag{14}$$

Measurements use either time-dependent gradient pulses or they combine static gradient fields with refocusing pulses. The resulting filter function is

$$F_t(\omega) = \frac{1}{2\pi}\left|\int_0^t dt' G(t')e^{-i\omega t'}\right|^2$$

and $G(t)$ is the field gradient modulated with the refocusing sequence.

Figure 11 compares the spectral density function 14 of a typical molecular diffusion process to the filter functions of various diffusion-weighting experiments. The resulting signal can be calculated from the comparison of different echo experiments. Optimising the parameters for these experiments allows very high-resolution k-sapce imaging [9], e.g. of human tissue. which maximises the diagnostic value of such experiments for a number of clinically relevant conditions. Additional details can be found in [9], which was published by partners from the PATHOS project. The optimisation of this approach is currently

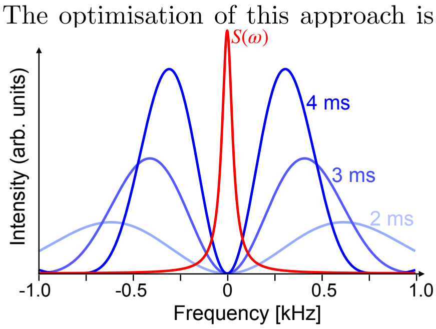

FIG. 11: Overlap of $F_t(\omega)$ with $S(\omega)$ (center) for gradient durations from 2 to 4 ms.

being explored by all partners of PATHOS, particularly in the WPs 2 and 3.

[1] D. Suter and G. A. Álvarez, Rev. Mod. Phys. **88**, 041001 (2016).

[2] G. Kurizki, G. A. Alvarez, and A. Zwick, Technologies **5**, 1 (2017).

[3] M. J. Biercuk, A. C. Doherty, and H. Uys, Journal of Physics B: Atomic, Molecular and Optical Physics **44**, 154002 (2011).

[4] G. A. Álvarez and D. Suter, Phys. Rev. Lett. **107**, 230501 (2011).

[5] T. Yuge, S. Sasaki, and Y. Hirayama, Phys. Rev. Lett. **107**, 170504 (2011), URL `http://link.aps.org/doi/10.1103/PhysRevLett.107.170504`.

[6] A. Zwick, G. A. Álvarez, and G. Kurizki, Phys. Rev. Applied **5**, 014007 (2016), URL `https://link.aps.org/doi/10.1103/PhysRevApplied.5.014007`.

[7] D. Goldwater, P. F. Barker, A. Bassi, and S. Donadi, Phys. Rev. Lett. **123**, 230801 (2019), URL `https://link.aps.org/doi/10.1103/PhysRevLett.123.230801`.

[8] P. A. Bottomley, T. H. Foster, R. E. Argersinger, and L. M. Pfeifer, Med Phys **11**, 425 (1984).

[9] A. Zwick, D. Suter, G. Kurizki, and G. A. Álvarez, Phys. Rev. Applied **14**, 024088 (2020), URL `https://link.aps.org/doi/10.1103/PhysRevApplied.14.024088`.

[10] J. E. Lang, D. A. Broadway, G. A. L. White, L. T. Hall, A. Stacey, L. C. L. Hollenberg, T. S. Monteiro, and J.-P. Tetienne, Phys. Rev. Lett. **123**, 210401 (2019), URL `https://link.aps.org/doi/10.1103/PhysRevLett.123.210401`.

[11] J. Zhang, S. S. Hegde, and D. Suter, Phys. Rev. A **98**, 042302 (2018), URL `https://link.aps.org/doi/10.1103/PhysRevA.98.042302`.

[12] J. Zhang, S. S. Hegde, and D. Suter, Phys. Rev. Applied **12**, 064047 (2019), URL `https://link.aps.org/doi/10.1103/PhysRevApplied.12.064047`.

[13] J. Zhang, S. S. Hegde, and D. Suter, arXiv:1911.06371 [quant-ph] (2019).

[14] S. S. Hegde, J. Zhang, and D. Suter, arXiv:1905.01649 [quant-ph] (2019).
[15] J. Clausen, G. Bensky, and G. Kurizki, Phys. Rev. Lett. **104**, 040401 (2010), URL `https://link.aps.org/doi/10.1103/PhysRevLett.104.040401`.
[16] J. Clausen, G. Bensky, and G. Kurizki, Phys. Rev. A **85**, 052105 (2012).
[17] A. G. Redfield, IBM Journal of Research and Development **1**, 19 (1957).
[18] G. Teklemariam, E. M. Fortunato, C. Lopez, J. Emerson, J. P. Paz, T. F. Havel, and D. G. Cory, Phys. Rev. A **67**, 062316 (2003).
[19] N. Bloembergen, E. Purcell, and R. Pound, Nature **160**, 475 (1947).
[20] N. Bloembergen, E. M. Purcell, and R. V. Pound, Phys. Rev. **73**, 679 (1948).
[21] R. Feynman, F. Vernon, and R. Hellwarth, J. Appl. Phys. **28**, 49 (1957).
[22] A. Kumar, G. Wagner, R. R. Ernst, and K. Wuethrich, J. Am. Chem. Soc. **103**, 3654 (1981).
[23] A. Kumar, R. C. R. Grace, and P. K. Madhu, Progr. NMR Spectrosc. **37**, 191 (2000).
[24] R. R. Ernst, The Journal of Chemical Physics **45**, 3845 (1966), https://doi.org/10.1063/1.1727409, URL `https://doi.org/10.1063/1.1727409`.
[25] J. S. Waugh, Journal of Magnetic Resonance (1969) **50**, 30 (1982), ISSN 0022-2364, URL `http://www.sciencedirect.com/science/article/B7GXD-4CRG961-17B/2/3d40cdb555cef42ef4f336320e566ae4`.
[26] D. Suter, K. Schenker, and A. Pines, J. Magn. Reson. **73**, 90 (1987).
[27] M. Novakovic, S. F. Cousin, M. J. Jaroszewicz, R. Rosenzweig, and L. Frydman, Journal of Magnetic Resonance **294**, 169 (2018), ISSN 1090-7807, URL `http://www.sciencedirect.com/science/article/pii/S1090780718301873`.
[28] A. L. Bloom and J. N. Shoolery, Phys. Rev. **97**, 1261 (1955), URL `https://link.aps.org/doi/10.1103/PhysRev.97.1261`.
[29] R. Ernst, G. Bodenhausen, and A. Wokaun, *Principles of nuclear magnetic resonance in one and two dimensions* (Oxford University Press, Oxford, 1987).
[30] E. Hahn, Phys. Rev. **80**, 580 (1950).
[31] I. Abella, N. Kurnit, and S. Hartmann, Phys. Rev. **141**, 391 (1966).
[32] A. G. Kofman and G. Kurizki, Phys. Rev. Lett. **87**, 270405 (2001), URL `http://link.aps.org/doi/10.1103/PhysRevLett.87.270405`.
[33] U. Haeberlen and J. Waugh, Phys. Rev. **175**, 453 (1968).
[34] U. Haeberlen and J. Waugh, Phys. Rev. **185**, 420 (1969).
[35] D. Suter and A. Pines, J. Magn. Reson. **75**, 509 (1987).
[36] H. Carr and E. Purcell, Phys. Rev. **94**, 630 (1954).
[37] S. Meiboom and D. Gill, Review of Scientific Instruments **29**, 688 (1958).
[38] L. Viola and S. Lloyd, Phys. Rev. A **58**, 2733 (1998).
[39] L. A. Zadeh, Proceedings of the IRE **50**, 856 (1962), ISSN 2162-6634.
[40] A. Einstein, Phys. Zeitschrift **18**, 121 (1917).
[41] M. Goldman, J. Magn. Reson. **149**, 160 (2001).
[42] R. Kimmich and E. Anoardo, Progress in Nuclear Magnetic Resonance Spectroscopy **44**, 257 (2004), ISSN 0079-6565, URL `http://www.sciencedirect.com/science/article/pii/S0079656504000196`.
[43] A. Ajoy, B. Safvati, R. Nazaryan, J. T. Oon, B. Han, P. Raghavan, R. Nirodi, A. Aguilar, K. Liu, X. Cai, et al., Nature Communications **10**, 5160 (2019), URL `https://doi.org/10.1038/s41467-019-13042-3`.
[44] F. Yan, S. Gustavsson, J. Bylander, X. Jin, F. Yoshihara, D. G. Cory, Y. Nakamura, T. P. Orlando, and W. D. Oliver, Nature Communications **4**, 2337 (2013), URL `https://doi.org/10.1038/ncomms3337`.
[45] J. Stepisnik, Physica B: Condensed Matter **183**, 343 (1993), ISSN 0921-4526, URL `http://www.sciencedirect.com/science/article/pii/092145269390124O`.
[46] P. T. Callaghan and J. Stepisnik, Journal of Magnetic Resonance, Series A **117**, 118 (1995), URL `http://www.sciencedirect.com/science/article/pii/S1064185885799597`.
[47] J. Stepsnik, S. Lasic, A. Mohoric, I. Sersa, and A. Sepe, Journal of Magnetic Resonance **182**, 195 (2006), ISSN 1090-7807, URL `http://www.sciencedirect.com/science/article/pii/S1090780706001819`.
[48] U. Haeberlen, in *Advances in magnetic resonance*, edited by J. Waugh (Acad. Press, New York, 1976), vol. Supplement 1 of *Advances in magnetic resonance*, chap. Supplement 1.
[49] M. G. A. Paris, Int. J. Quantum Technology **7**, 125 (2009).
[50] G. A. Álvarez, D. D. B. Rao, L. Frydman, and G. Kurizki, Phys. Rev. Lett. **105**, 160401 (2010), URL `https://link.aps.org/doi/10.1103/PhysRevLett.105.160401`.
[51] C. O. Bretschneider, G. A. Álvarez, G. Kurizki, and L. Frydman, Phys. Rev. Lett. **108**, 140403 (2012), URL `http://link.aps.org/doi/10.1103/PhysRevLett.108.140403`.
[52] M. Lovric, H. G. Krojanski, and D. Suter, Phys. Rev. A **75**, 042305 (pages 8) (2007), URL `http://link.aps.org/abstract/PRA/v75/e042305`.
[53] L. Cywiński, R. M. Lutchyn, C. P. Nave, and S. Das Sarma, Phys. Rev. B **77**, 174509 (2008), URL `https://link.aps.org/doi/10.1103/PhysRevB.77.174509`.
[54] P. Szańkowski, Phys. Rev. A **100**, 052115 (2019), URL `https://link.aps.org/doi/10.1103/PhysRevA.100.052115`.
[55] J. Zhang, X. Peng, N. Rajendran, and D. Suter, Phys. Rev. A **75**, 042314 (pages 8) (2007), URL `http://link.aps.org/abstract/PRA/v75/e042314`.
[56] M. Wolf, A. de Boer, K. Sharma, P. Boor, T. Leiner, G. Sunder-Plassmann, E. Moser, A. Caroli, and N. P. Jerome, Nephrol. Dial. Transplant. **33**, ii41 (2018).
[57] K. W. Chan, W. Huang, C. H. Yang, J. C. C. Hwang, B. Hensen, T. Tanttu, F. E. Hudson, K. M. Itoh, A. Laucht, A. Morello, et al., Phys. Rev. Applied **10**, 044017 (2018), URL `https://link.aps.org/doi/10.1103/PhysRevApplied.10.044017`.
[58] G. A. Paz-Silva and L. Viola, Phys. Rev. Lett. **113**, 250501 (2014), URL `https://link.aps.org/doi/10.1103/PhysRevLett.113.250501`.
[59] K. C. Young and K. B. Whaley, Phys. Rev. A **86**, 012314 (2012), URL `https://link.aps.org/doi/10.1103/PhysRevA.86.012314`.
[60] Y. Romach, C. Müller, T. Unden, L. J. Rogers, T. Isoda, K. M. Itoh, M. Markham, A. Stacey, J. Meijer, S. Pezzagna, et al., Phys. Rev. Lett. **114**,

017601 (2015), URL https://link.aps.org/doi/10.1103/PhysRevLett.114.017601.
[61] C. A. Meriles, L. Jiang, G. Goldstein, J. S. Hodges, J. Maze, M. D. Lukin, and P. Cappellaro, J. Chem. Phys. **133**, 124105 (2010), ISSN 00219606, URL http://dx.doi.org/doi/10.1063/1.3483676.
[62] J. T. Muhonen, J. P. Dehollain, A. Laucht, F. E. Hudson, R. Kalra, T. Sekiguchi, K. M. Itoh, D. N. Jamieson, J. C. McCallum, A. S. Dzurak, et al., Nat Nano **9**, 986 (2014).
[63] O. E. Dial, M. D. Shulman, S. P. Harvey, H. Bluhm, V. Umansky, and A. Yacoby, Phys. Rev. Lett. **110**, 146804 (2013), URL https://link.aps.org/doi/10.1103/PhysRevLett.110.146804.
[64] F. Yoshihara, Y. Nakamura, F. Yan, S. Gustavsson, J. Bylander, W. D. Oliver, and J.-S. Tsai, Phys. Rev. B **89**, 020503 (2014), URL https://link.aps.org/doi/10.1103/PhysRevB.89.020503.
[65] J. Bylander, S. Gustavsson, F. Yan, F. Yoshihara, K. Harrabi, G. Fitch, D. G. Cory, Y. Nakamura, J.-S. Tsai, and W. D. Oliver, Nature Physics **7**, 565 (2011), URL https://doi.org/10.1038/nphys1994.
[66] S. Kotler, N. Akerman, Y. Glickman, and R. Ozeri, Phys. Rev. Lett. **110**, 110503 (2013), URL https://link.aps.org/doi/10.1103/PhysRevLett.110.110503.
[67] A. Soare, H. Ball, D. Hayes, J. Sastrawan, M. C. Jarratt, J. J. McLoughlin, X. Zhen, T. J. Green, and M. J. Biercuk, Nature Physics **10**, 825 EP (2014).
[68] T. Green, H. Uys, and M. J. Biercuk, Phys. Rev. Lett. **109**, 020501 (2012), URL https://link.aps.org/doi/10.1103/PhysRevLett.109.020501.
[69] L. M. Norris, G. A. Paz-Silva, and L. Viola, Phys. Rev. Lett. **116**, 150503 (2016), URL https://link.aps.org/doi/10.1103/PhysRevLett.116.150503.
[70] L. Viola, E. M. Fortunato, M. A. Pravia, E. Knill, R. Laflamme, and D. G. Cory, Science **293**, 2059 (2001).
[71] Y. Sung, F. Beaudoin, L. M. Norris, F. Yan, D. K. Kim, J. Y. Qiu, U. von Lüpke, J. L. Yoder, T. P. Orlando, S. Gustavsson, et al., Nature Communications **10**, 3715 (2019).
[72] S. Berger and S. Braun, *200 and More NMR Experiments* (Wiley, 1998).
[73] G. S. Uhrig, New Journal of Physics **10**, 083024 (2008), URL http://stacks.iop.org/1367-2630/10/i=8/a=083024.
[74] A. Ghosh and A. Kumar, J. Magn. Reson. **173**, 125 (2005).
[75] S. S. Hegde and T. S. Mahesh, Phys. Rev. A **89**, 062317 (2014).
[76] Y. Pan, Z.-R. Xi, and J. Gong, Journal of Physics B: Atomic, Molecular and Optical Physics **44**, 175501 (2011).
[77] R. Kachru, T. Mossberg, and S. Hartmann, J.Phys.B **13**, L363 (1980).
[78] P. W. Anderson, Phys. Rev. **76**, 647 (1949).